Particle Accelerators, 1995, Vol. 51, pp. 135–154
Reprints available directly from the publisher
Photocopying permitted by license only

THREE DIMENSIONAL KLYSTRON SIMULATION

ULRICH BECKER,[1] MARTIN DOHLUS[2] and THOMAS WEILAND[1]

[1]*Technische Hochschule Darmstadt, Fachbereich 18,*
Fachgebiet Theorie Elektromagnetischer Felder,
Schloßgartenstraße 8, D-64289 Darmstadt, Germany

[2]*Deutsches Elektronen Synchroton, DESY, Notkestraße 85,*
D-22603 Hamburg, Germany

(Received 8 May 1995; in final form 27 July 1995)

The development of high power klystrons requires computer codes simulating the complex interaction of electrons with the electromagnetic field as realistically as possible. We present a three dimensional computer simulation of a klystron output circuit including fully relativistic particle dynamics. The power extraction is simulated with the realistic waveguide geometry bounded by a broadband waveguide boundary condition. The data base for the injection of the beam in the output circuit is derived from the steady state solution of a two dimensional simulation of the first klystron cavities. The interface between rotationally symmetric and nonsymmetric part includes not only the particle parameters but also the electromagnetic field at the interface plane. Results are presented for a 150 MW S-band klystron, which was designed and built at the Stanford Linear Accelerator Center (SLAC) as a part of an international collaboration with Deutsches Elektronen Synchrotron (DESY). The simulations were performed by using the electromagnetic simulator MAFIA.

KEY WORDS: Klystrons, RF sources, particle in cell codes, computer simulation

1 INTRODUCTION

Future e^+e^- linear colliders must provide a center of mass energy in the range of 0.3 to 1 TeV to be of interest for high energy physics. Today several possibilities to build such a linear collider are under investigation, which mainly differ in the operation frequency. At Deutsches Elektronen Synchrotron (DESY) the feasibility of a S-band solution is studied (S-Band Linear Collider: SBLC). To achieve the desired collision energy a huge number of RF power sources will be needed along the accelerator. Thus the research on these sources, namely the klystrons, is one of the main topics. In order to get a better understanding of the complex particle dynamics inside a klystron and to optimize its parameters, accurate simulation tools are necessary.

With exception of the input and output cavities the klystron in Figure 1a has a pure symmetry of revolution. For the fields and the particles a pure monopole behaviour is desired.

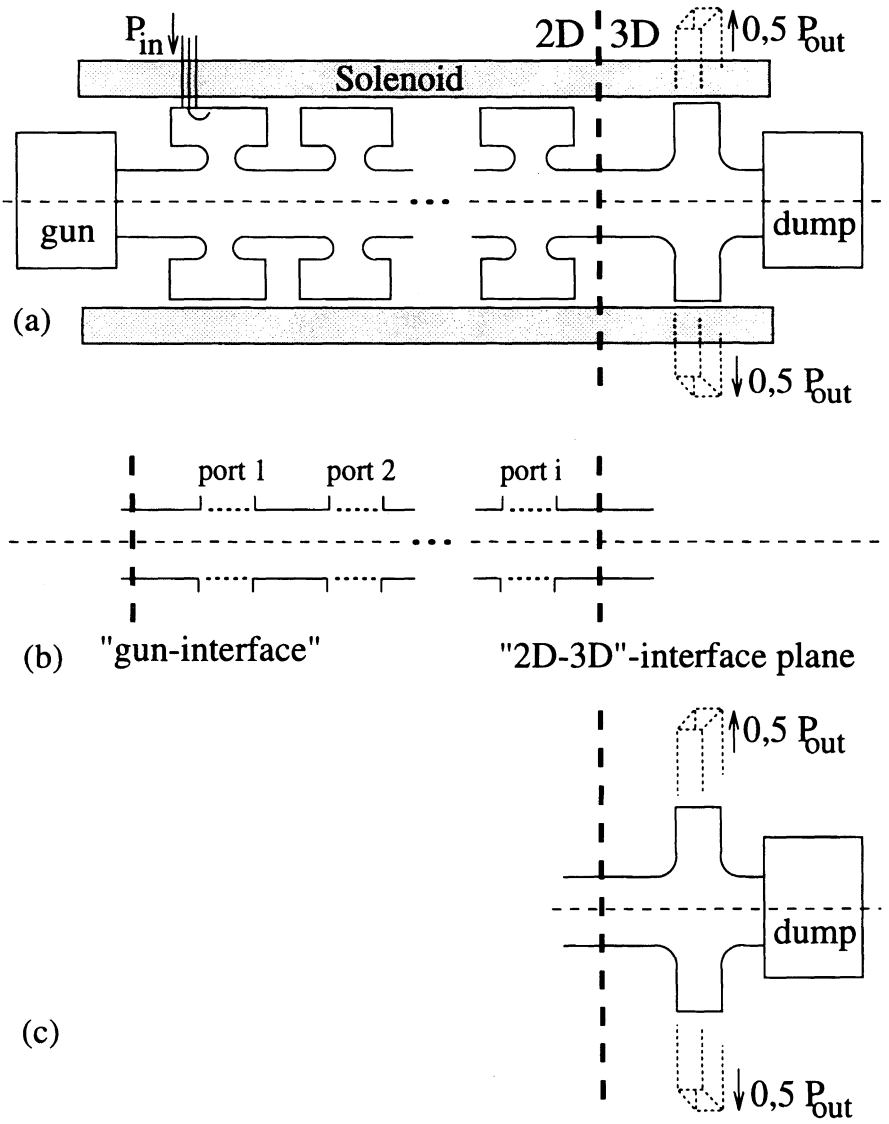

FIGURE 1: (a) Schematic diagram of a klystron with a symmetrical double output waveguide, (b) Two dimensional klystron simulation, setup with interface to gun data, port approximations and infinite beam pipe behind the "2D–3D"-interface plane, (c) The three dimensional part is stimulated by boundary fields and particles as they are monitored in the 2D simulation.

Unless the fields with higher azimuthal orders are not stimulated too strongly by the corresponding statistical contributions of the gun current, and if the higher order cavity modes are not reduced in damping or even amplified by the beam loading, the assumption of rotational symmetry is reasonable for most parts of the klystron. The symmetry of revolution of the input cavity is slightly disturbed by the coupling loop to the coaxial input transmission line. As this cavity is operated in the linear regime, the spectral characteristic of the stimulation ensures that only the fundamental mode is excited. For the further discussion, the small contribution of non-monopole fields in the input cavity shall be neglected. However, the output cavity has one or two major coupling holes which cause significant asymmetries in the field distribution. The following aspects make a treatment of this output cavity rather difficult:

- The field-particle interaction is in a nonlinear regime if the klystron is operated close to saturation.
- The beam current has a wide frequency spectrum and thus excites higher order modes.
- The low external Q-value of the output cavity causes a much stronger perturbation of the monopole fields than in the input cavity. Furthermore the frequency selectivity is reduced due to the low quality factor.

If the output cavity has two waveguides and maintains two planes of symmetry (e.g. $\varphi = 0$, $\varphi = \pi/2$) the dipole contribution vanishes. Therefore pure monopole calculations could be very good approximations if higher order monopole fields could be taken into account. This is not a trivial task because the monopole properties of the 3D cavity fields (in presence of the waveguides) have to be evaluated and simulated for all spectral components. 3D cavity simulation overcomes this problem in a natural way, allows the calculation of more general geometries and enables a true calculation of intersecting particles and surface gradients of electric fields. These values are important e.g. to investigate whether the field emission limit is already reached.

A fully 3D simulation of the whole klystron takes a long time. Inside the code MAFIA features are available to simulate the output circuit in xyz-geometry including all effects mentioned above. Therefore an interface between the two dimensional particle-in-cell (PIC) code TS2 and the three dimensional PIC-code TS3 has been developed, which stores all necessary data of particles and fields in rz-geometry to reinitialize them in xyz-run, as shown schematically in Figure 1c. A detailed description of this interface is given in Section 3.

TABLE 1: Design specifications for the 150 MW S-band klystron.

Beam voltage	535 kV
Beam current	700 A
RF Pulseduration	3 μs
RF Output Power	150 MW
Saturated Gain	$\approx$55 dB
Efficiency	>40 %
Operation Frequency	2998 MHz

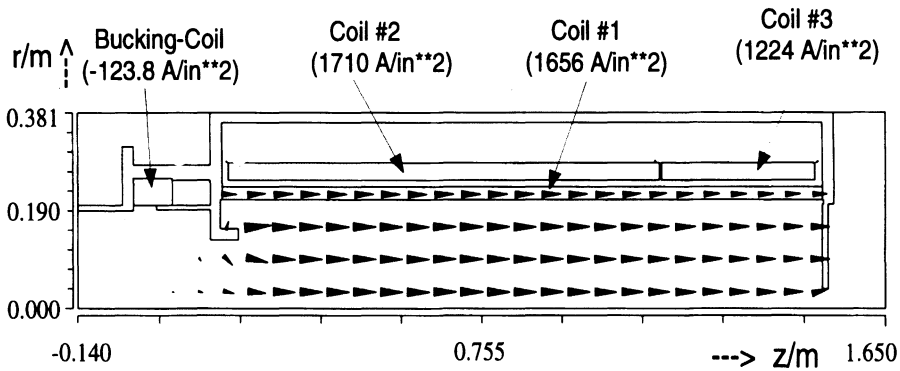

FIGURE 2: The complete magnetic structure including a plot of the solenoid field, used for all PIC-simulations presented in this paper. The maximum field value is 0.19 Tesla. The length z defines the distance from the cathode surface along the drift tube.

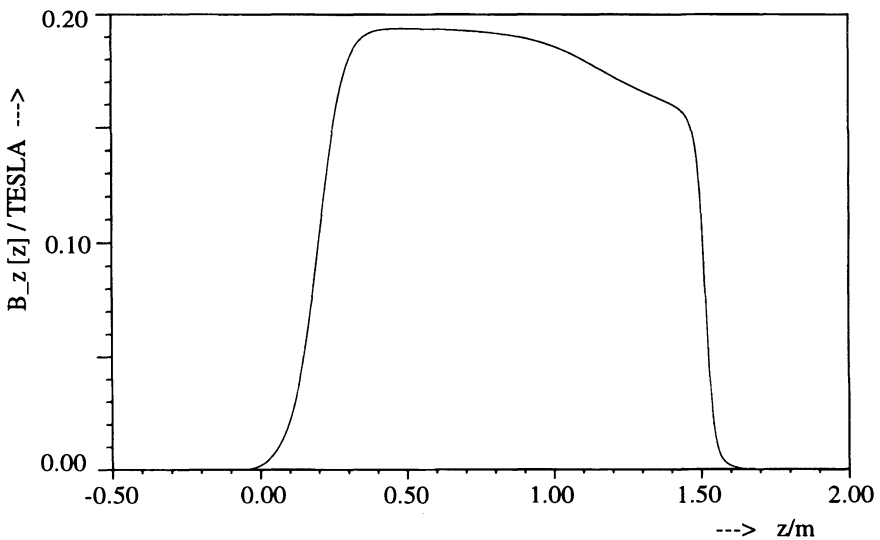

FIGURE 3: z-component of the static magnetic field on axis, calculated with the Statics-Solver S of MAFIA. The surface of the cathode is located at $z=0m$.

The features developed are illustrated with specific examples for a 150 MW S-band klystron,[1] assigned as RF power source for the SBLC test facility. This klystron employs seven cavities, input and output cavity included. It has a total length from the gun baseplate to the collector tip of 104 inches. The maximum diameter of the solenoid coil is 15 inches. The first klystron was built and successfully processed at the Stanford Linear Accelerator Center (SLAC). Its design specifications are listed in Table 1.

2 TWO DIMENSIONAL ANALYSIS

In order to obtain the input data for the 3D calculation, some rotationally symmetric parts of the klystron are simulated in rz-geometry.

2.1 Solenoid field

The complete magnetic structure, consisting of four axisymmetric coils and the iron core, is shown in Figure 2. In addition the values of the assumed current density are given in this figure. The static magnetic field, calculated with the Statics-Solver S of MAFIA, can be loaded into the different rz- and xyz-meshes of the PIC-simulations. Afterwards the divergence of the loaded field is checked to guarantee its physical correctness.

2.2 Cavity parameter

The cold cavity parameters, needed for the 2D PIC-simulation, are calculated with the Eigenmode Solver E and the Postprocessor P of MAFIA. In order to calculate accurate values for the resonance frequencies (error less than 1 MHz), which is very important especially for the first cavities, it is necessary to choose a smooth approximation of the gap noses by triangular cells.[8] The typical geometry of the first six cavities is shown in Figure 4. In Table 2 the cold cavity parameters are listed, as they are used in the two dimensional PIC-simulation.

2.3 Pic simulation of DC-current

The PIC-simulation starts right behind the gun region, where the DC-current is reinjected. At the injection plane the tangential electric field is derived for a pure DC-current. Thus one prevents a de- or accelerating effect by the boundary on the electron beam. The properties of the incoming particles are calculated with the code EGUN,[4] applying different DC-gun voltages. A microperveance of roughly 1.8 was obtained, depending slightly on the gun voltage.

TABLE 2: Cold cavity parameters of the fundamental cavity modes of the 150 MW S-band klystron. The parameters listed are the loaded quality factor Q_e, the resonance frequency f_o and the loss-independant ratio between shunt impedance and quality factor R/Q. The frequencies are calculated by the Eigenmode Solver E, the shunt impedances and the Q-values by the Postprocessor P of MAFIA.

Cavity	Q_e	f_o/GHz	$(R/Q)/\Omega$
1	127	2.998	86.7
2	8247	3.006	89.0
3	8314	3.023	91.6
4	8868	3.174	106.5
5	7491	3.445	98.1
6	9492	3.384	126.5
7	14	2.998	132.7

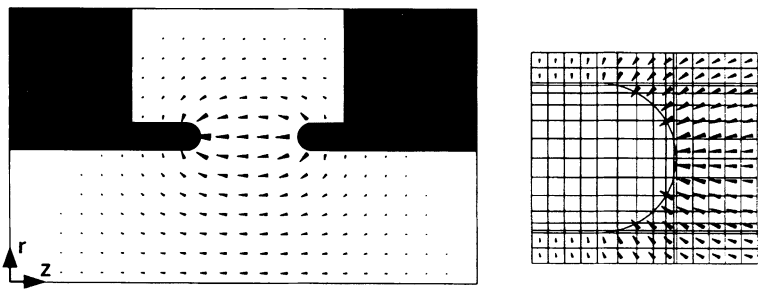

FIGURE 4: Typical field pattern of the electric field vector of the fundamental mode in one of the first six cavities. The zoom-in view of the gap nose region illustrates the smooth approximation of the circle by a triangular filling of the grid cells. By this approximation we reach high accuracy for the resonance frequency, well below 1 MHz.

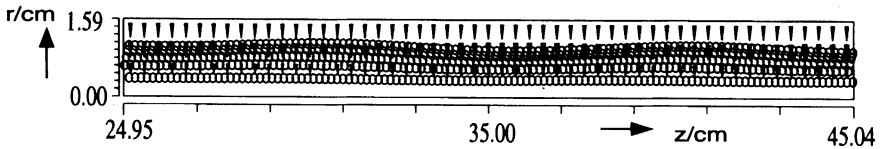

FIGURE 5: The electric field of the DC-beam simulation inside the tube with macro particles after 10 ns (approximately 30 RF-periods). The length z defines the distance from the cathode surface along the drift tube. The scalloping of the beam envelope is caused by the helical movement of the electrons in the longitudinal magnetic field.

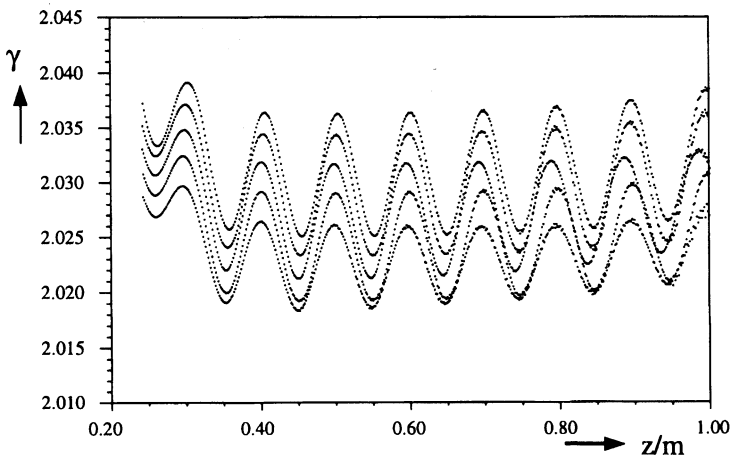

FIGURE 6: The particle energy along the drift tube after 10 ns (approximately 30 RF-periods). For a DC-gun voltage of 535 kV the incoming particles at the gun interface have γ-values in the range 2.029 to 2.038. This corresponds to DC-voltages between 526 kV and 530 kV. From this plot one can estimate the scalloping wavelength in the solenoid field to be approximately 10.5 cm.

When starting the PIC-simulation one has to guarantee a smooth simulation of the DC-current inside the tube without cavity interaction. The high frequency noise, caused by the interpolation of the particle movement to the current density vector and summed up in every step of the time integration, has to be small compared to the other fields even after 30 RF-periods simulation time. To reach a smooth DC-current simulation the following points are applied:

- To simulate the DC-beam with macro particles, it is necessary to use a systematic injection scheme, meaning the simulation of a certain number of "rays" over the beam cross-section. In each ray the time delay between two following particles is constant (see Figures 5 and 6).
- A "half-Gaussian" function is used as time function for the switching-on of the current to prevent the stimulation of waveguide modes.
- A spatial filter is applied on the current density and the electromagnetic field used for the calculation of forces acting on the particles. This filter damps unphysical high frequency noise. It maintains the continuity equation, which is *a priori* satisfied in the FIT algorithm (Finite Integration Technique).[3]

The high quality of the DC-current simulation, even after 30 RF-periods simulation time, is illustrated in the plot of the particle energy (Figure 6).

2.4 *Port approximation*

The real time to reach the steady state solution of an excitated cavity mode (in amplitude and phase) depends directly on the quality factor of this particular mode. Due to the high quality factors (> 100) for the modes of closed reentrance cavities, the time to build-up the mode ranges from hundred to a few thousand RF-periods. A realistic simulation of this process would take too long cpu time. For this reason the interaction of the cavities with the high energy particle beam is simulated with the port approximation,[5] which speeds up the time to reach the steady state solution for the klystron. In this method the electromagnetic field inside the cavity is replaced by a controlled excitation of the fundamental cavity mode. At the position of the gap the oscillating electric field of the fundamental mode is bounding the tube. This procedure has the advantage that the amplitude and the phase of the mode can be adjusted during the PIC-simulation by varying the boundary fields. Therefore the steady state solution for all cavities can be iterated in a few RF-periods despite the high Q values. The cavity impedance

$$\underline{Z}(f) = \frac{R}{Q} \cdot \left(\frac{1}{Q_e} + 2j \frac{f - f_o}{f} \right)^{-1}$$

defines the relation in steady state between cavity voltage and induced current, both given as complex amplitudes in frequency domain. Here f is the operating frequency, f_o the resonance frequency of the particular mode, R/Q the ratio between shunt impedance and quality factor and Q_e the external quality factor.

The induced current is derived from the power exchange between cavity mode and beam

$$P(t) = \int_{V_{\mathrm{Cav}}} \vec{J}(r, z, t) \cdot \vec{E}_M(r, z)\, dV$$

with

V_{Cav} : cavity volume

$\vec{J}(r, z, t)$: current density of the beam

$\vec{E}_M(r, z)$: electric mode pattern, peak value of axis voltage is 1 Volt

The corresponding complex amplitude at the driving frequency can be written as

$$P(t) \quad \circ\!\!-\!\!\bullet \quad \underline{\hat{p}} = \underline{\hat{i}}_{\mathrm{ind}} \cdot 1\,\mathrm{V}$$

In the following paragraph the current density is split into its time independent (DC) and time dependent content (AC). The most critical part of the simulation concerning signal-to-noise ratio is the particle-field-interaction in the first cavities where the AC-component of current is small compared to the total current. Therefore these cavities are treated with small signal approach which allows to split the induced current into an input (caused by incoming AC-components of the beam) and a beam loading part. The beam loading admittances are derived in a separate PIC run by calculating the induced current in each cavity for an incoming pure DC-current. This precalculation of beam loading admittances $\underline{Y}_{bl}$, as listed in Table 3, is necessary to realize linear approach and to derive the axis voltage in cavity #1 from the drive power level. The small signal approach leads to good results up to a cavity voltage of half the DC-beam voltage.

For cavities with axis voltages in the range of the DC-beam voltage, the steady state voltage, of the cavity mode is found by a relaxation method:[6] in every time step the amplitude of the mode is corrected until the complex cavity equation $\underline{\hat{u}} = \underline{Z}\, \underline{\hat{i}}_{\mathrm{ind}}$ is fulfilled with a certain accuracy.

The harmonic content of the beam current in steady state for the two dimensional simulation is shown in Figure 7.

TABLE 3: Beam loading admittances $\underline{Y}_{bl}$ for a DC-beam voltage of 535kV.

Cavity	$\underline{Y}_{bl}/\mu\mathrm{S}$
1	64.2 – j 3.08
2	60.2 – j 1.49
3	58.1 – j 2.23
4	65.1 – j 6.21
5	59.2 – j 6.17
6	61.1 – j 7.78
7	68.3 – j 15.6

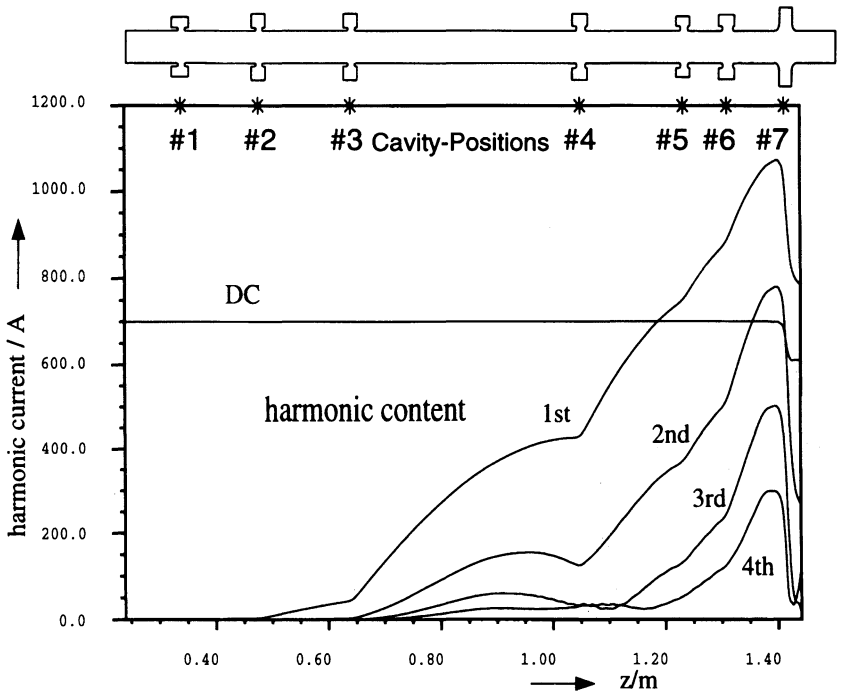

FIGURE 7: Harmonic content of the current along the klystron tube. The solution is found with a two dimensional PIC-simulation for a drive power of 200 W in cavity #1. The DC-input power is 535 kV·700 A. The stars on top of the plot mark the center locations of the cavity gaps.

3 TRANSITION FROM TWO TO THREE DIMENSIONS

In order to study higher order modes and other unsymmetrical effects in the output cavity caused by the strong coupling to the external waveguides, the klystron output circuit is simulated with a 3D PIC-code. Therefore a data transfer from the 2D to the 3D simulation is necessary. The most realistic way of doing this is to store the particle and field information for one RF-period in steady state at a particular z-position. The separation into a pure rotationally symmetric part (rz-structure) and a 3D part (xyz-structure) is possible if the beampipe between the last cavity of the first part and the first cavity of the second part is long enough, so that all cavity fields can be neglected in the interface plane. Additionally we assume, that all particles travel only in one direction (from the 2D to the 3D part). The validity of this assumption can be checked during the simulation by counting the particles moving backward and hitting the interface plane.

In the rz-simulation of the rotationally symmetric part the 3D structure is replaced by a straight beampipe. In the ideal case, this pipe has infinite length and the field of all particles that passed the interface plane vanishes at a certain distance from the interface plane. In the

real calculation the beampipe has a finite length and is terminated by an absorbing boundary. It is possible to make the pipe long enough that boundary reflections can be neglected in the interface plane for spectral components below the cutoff frequency (≈7.3 GHz in the beampipe of the S-band klystron).

When steady state is reached the particle statistics and the field components are stored over one period in the interface plane.

On the 3D side of the interface plane particles have to be started and a boundary field has to be stimulated. The aim is to initialize the same periodic behaviour as on the 2D side and thus to be able to calculate the resulting three dimensional particle dynamics and the induced electromagnetic fields. Concerning this reinitialisation one has to take care of the following points:

- There is no one-to-one correspondence between the "2D-particles" and the "3D-particles". A two dimensional macro particle is localized in the rz-plane. The corresponding three dimensional charge distribution has the shape of a ring, but the three dimensional PIC-code simulates point charges.
- The initial boundary value problem is completely determined by one tangential boundary field (either electric $\vec{E}_t$ or magnetic $\vec{B}_t$ field) and the internal sources, namely the currents due to the moving particles. This is true if the exact boundary field is applied over the entire time range including the transient process. An unphysical static field can be induced, if only the stored periodic field is switched on with no special care to the transients.
- The boundary field of the two dimensional calculation has to be interpolated to the grid of the three dimensional calculation. Interpolation errors can cause unphysical longitudinal components of the static magnetic field rising linearly with time.

In the time integration by leap frog algorithm the divergence of the $\vec{E}$- and $\vec{B}$-fields are independent of the boundary fields. Therefore the divergence of the electric field is directly related to the stimulating current density field. The continuity is fulfilled if the particle motion is mapped to a consistent current density field for all time steps of the integration.

3.1 The particle interface

When steady state in the two dimensional PIC-simulation is reached during one RF-period the following parameters are stored for each macro particle crossing the interface plane:

- r_i: radial position.
- $p_{r,i}$, $p_{\varphi,i}$, $p_{z,i}$: the vector of momentum.
- t_i: time of crossing the interface plane.

According to the time of crossing the interface plane each 2D macro particle (ring-particle) with the charge Q_{2D} is split into $4 \cdot n$ ($n \in N$) 3D macro particles (point-particles) with $Q_{3D} = Q_{2D}/(4n)$. This "splitting-ratio" is chosen to prevent the excitation of dipole modes by statistical effects in the particle interface. The positions of the 3D particles are equispaced along the original 2D ring and the momenta are set to the momenta of the corresponding

sub rings. This azimuthal segmentation is done with an individual reference angle for every 2D particle and for each reinjection after a full RF-period. Thus systematic errors can be avoided.

During the first RF-periods, the charges of the 3D macro particles are smoothly increased to reduce the unwanted spectral components of the switching process. Thus the charge injected at the time t into in the 3D simulation is calculated as

$$Q_{\text{used}}(t) = Q_{3D} \cdot f(t) = \frac{Q_{2D}}{(4n)} \cdot f(t)$$

with

$$f(t) = \begin{cases} 0 & ; \quad t \leq 0 \\ (t/T_{\text{on}})^3 \left[6(t/T_{\text{on}})^2 - 15(t/T_{\text{on}}) + 10\right] & ; \quad 0 < t \leq T_{\text{on}} \\ 1 & ; \quad T_{\text{on}} < t \end{cases}$$

Here T_{on} is the switching time. Neither the position or momentum vector nor the time of injection is mapped to any regular grid.

3.2 *The field interface*

From the two dimensional calculation the following field information is passed to the three dimensional solver:

- period length T and the number of 2D time steps for one RF-period n_T.
- description of the boundary mesh.
- tangential electric field components for all time steps of a steady state period (synchronized to the particle storage) and the mean value of the longitudinal magnetic field at all boundary points.

Before performing the spatial interpolation and creating the transient switching field the 3D time steps have to be adjusted to the value of the 2D calculation. Therefore the 2D time steps have to fulfill the 3D stability criterion of the leap frog integration. Usually this causes no significant rise of the computational effort so that it is not necessary to compute with different time steps and to map the sampled fields by a Fourier expansion to another time grid.

The tangential electric boundary field is turned on smoothly with the following time dependency:

$$\vec{E}_{3D}(t) = \vec{E}_P'(t) \cdot f(t) + \vec{E}_S' \cdot \dot{f}(t)$$

Here $f(t)$ is the same switching function as defined for the particle interface (see subsection 3.1) and $\dot{f}(t)$ its time derivative.

The electric field $\vec{E}_P'(t)$ is the periodical extension of the interpolated boundary field and $\vec{E}_S'$ is required to induce the correct DC-component of the normal magnetic field. These fields have to fulfill the following equations:

$$\int_0^T \text{rot}\, \vec{E}_P'(t) \cdot \vec{e}_z \, dt = 0$$

$$\bar{B}_z = \frac{1}{T} \int_{\tilde{t}>T_{on}}^{\tilde{t}+T} B_z(t)\, dt = -\frac{1}{T} \int_{\tilde{t}>T_{on}}^{\tilde{t}+T} \int_0^t \text{rot}\, \vec{E}_{3D}(\tau) \cdot \vec{e}_z \, d\tau \, dt$$

The first equation could be violated if the 2D calculation did not reach steady state or if the field is interpolated without maintaining this physical property. Therefore we split the 2D field into a pure DC-part and a pure AC-part. For the DC-part a potential function is calculated and interpolated to each 3D boundary point. The field $\vec{E}_P'(t)$ is the sum of the gradient of this function and the conventional interpolated AC-part.

The second equation leads directly to a partial differential equation for $\vec{E}_S'$:

$$\bar{B}_z = \text{rot}\, \vec{E}_S' \cdot \vec{e}_z \underbrace{\left(-\frac{1}{T} \int_{\tilde{t}>T_{on}}^{\tilde{t}+T} \int_0^t \dot{f}(\tau)\, d\tau \, dt \right)}_{=-1} + \cdots$$

$$\cdots + \underbrace{\left(-\frac{1}{T} \int_{\tilde{t}>T_{on}}^{\tilde{t}+T} \int_0^t f(\tau)\, \text{rot}\, \vec{E}_P'(\tau) \cdot \vec{e}_z \, d\tau \, dt \right)}_{=+G}$$

$$\text{rot}\, \vec{E}_S' \cdot \vec{e}_z = G - \bar{B}_z$$

The integration of G is performed numerically. The one degree of freedom in the calculation of $\vec{E}_S'$ was used to maintain the monopole symmetry:

$$\vec{E}_S' = E_S'(r) \cdot \vec{e}_\varphi$$

4 THREE DIMENSIONAL ANALYSIS

4.1 Description of the three dimensional PIC code

The three dimensional PIC code computes the time integration of electromagnetic fields selfconsistently with the time integration of the equations of motion of charged particles that move under the influence of those fields. Since the fields caused by the moving charges are also taken into account, effects like space charge and magnetic forces between particles are fully simulated. In the program a nonequidistant cartesian grid is used with the possibility of triangular filling of meshcells.[3]

The discretization of Maxwell's equations using the Finite Integration Technique (FIT) yields a set of discrete matrix equations.[7] The discrete operators used in the FIT show some important analogies with algebraic operators which are very helpful to check analytic properties of the calculated electromagnetic fields. The time derivative is substituted by a discrete differential operator of second order. The well-known leap-frog scheme is applied for the time integration of the fields, the particle positions and momenta. The discrete continuity equation is a priori fulfilled by using an algorithm of Buneman and Pardo[12] which calculates only divergence-free current densities on the grid lines.

In a real klystron rectangular waveguides are strongly coupled to the output cavities guiding the RF energy away. Such waveguides can be realized by means of a broadband waveguide-boundary-condition.[9] This boundary treatment allows correct broadband computation of the amplitudes of all modes in the waveguides as excited by the beam in the cavity. A broadband boundary operator is used which is based on the decomposition into waveguide modes and a one dimensional propagation model for each mode. The 1D operators perform the propagation of the different waveguide modes at the boundary plane in large frequency ranges. This sophisticated boundary condition shows reflection factors as low as -110dB (for single precision calculations).

4.2 Simulation results

In this section we present the simulation results for the output cavity of the 150 MW S-band klystron, briefly described in the introduction. The interface plane is located approximately in the middle between the last two cavities. The distance between the interface plane and a neighboured cavity gap has a length of 5 cm which is more than three times the tube radius. Thus cavity modes can be neglected at the interface plane.

Particles which are backscattered from the Output Cavity to the interface plane can be detected by a dedicated monitor. Only for the drive levels 400 W and 500 W at a DC-gun voltage of 535 kV backwards travelling particles could be observed during the simulation. The power loss of those reflected particles in the interface plane is less than 30 kW and thus can be neglected.

Figures 8 and 9 show the geometry of the simulation area. Although the output cavity is symmetrical with respect to the $x = 0$ and $y = 0$ plane we did not make use of this symmetry as one normally does in RF mode computation. The reasons for using the fullsize model are:

- The helical movement of the electrons in the longitudinal magnetic field is not symmetrical. Thus a magnetic boundary condition would simulate unphysical mirror charges. In other words, the electromagnetic field of the beam-current fulfills neither an electric nor a magnetic boundary condition.

- The excitation of many cavity modes would be disabled by restricting the number of existing modes due to a symmetry condition at $x = 0$ and $y = 0$. Studying all higher order modes was one of the main reasons to perform the 3D PIC-simulation of the output cavity.

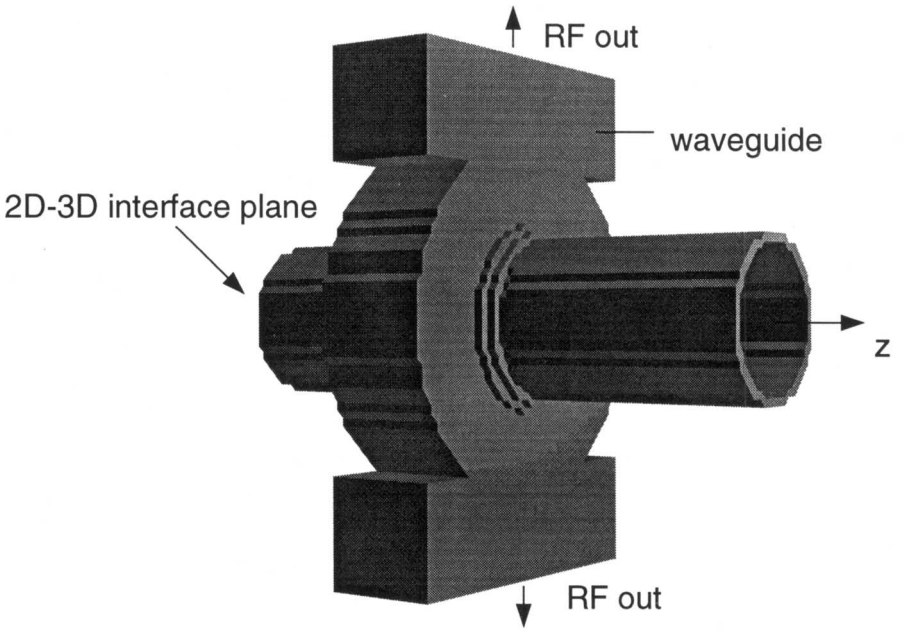

FIGURE 8: This plot shows the simulation volume around the output cavity studied with the 3D PIC simulation. The volume is discretized with 206,241 meshpoints.

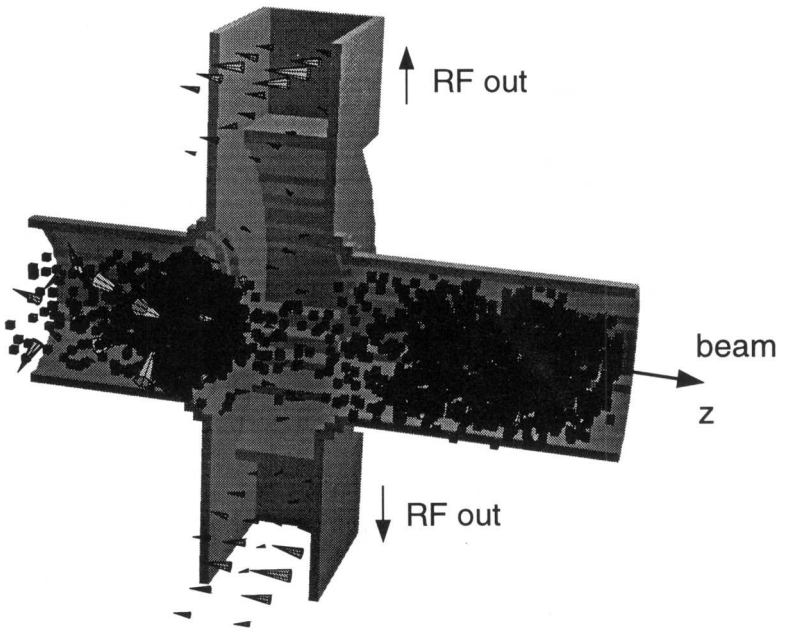

FIGURE 9: Electric field and particle positions in the region around the output cavity. On the left side the interface plane is located where the particle parameters and the field values are derived from the two dimensional PIC-simulation.

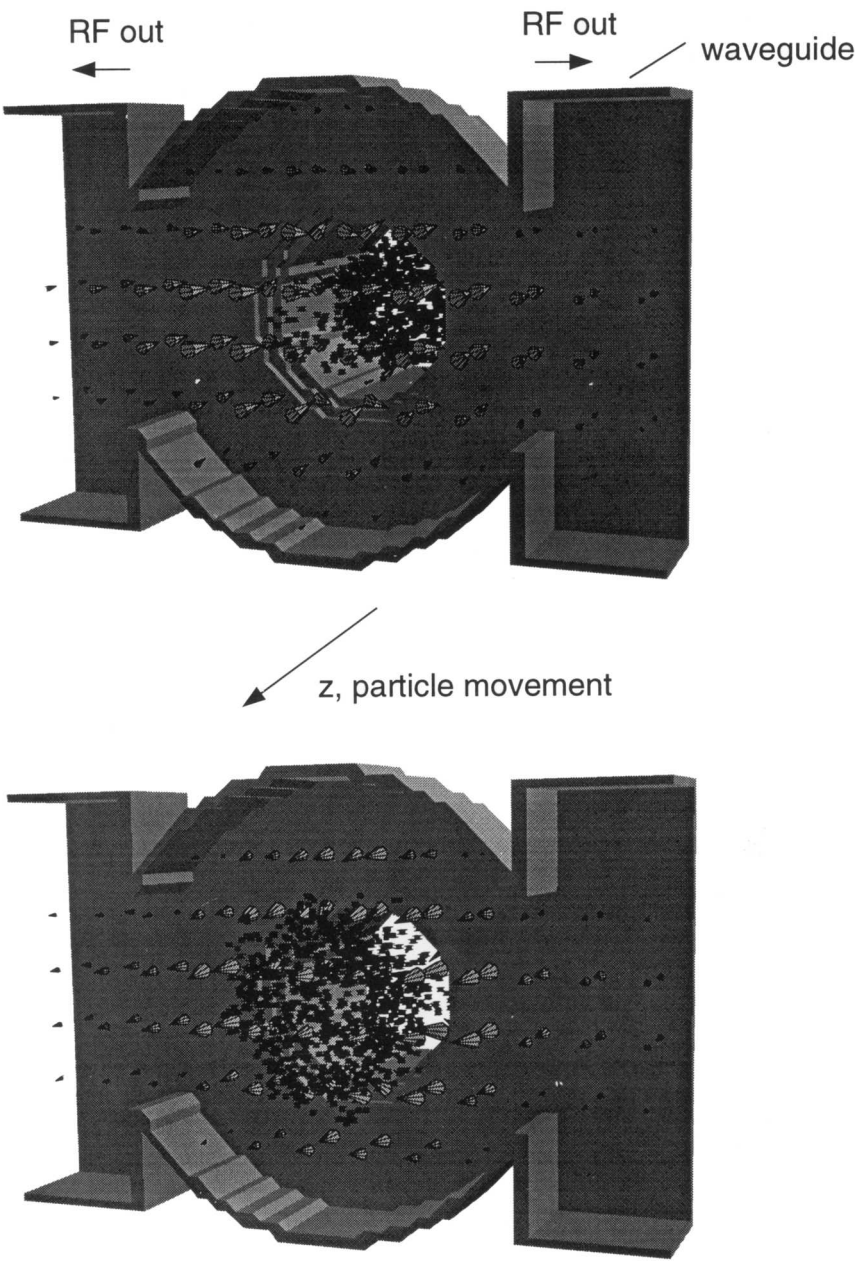

FIGURE 10: Electric field vector and the corresponding particle-positions at two time steps shifted by a half RF-period in steady state. The particles move out of the paper plane. Obviously the electric field in the lower picture decelerates the particles moving in the core of the cavity.

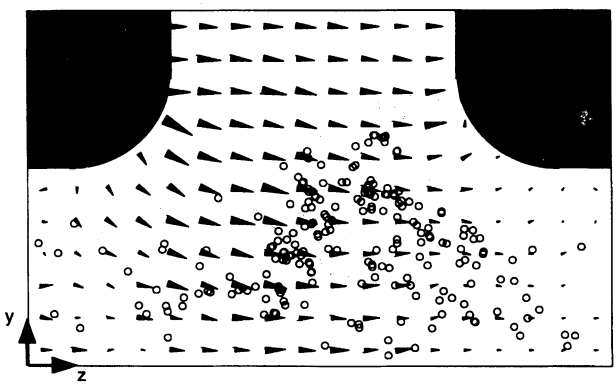

FIGURE 11: Electric field vector and particle positions in one part of the $x = 0$ plane of the 3D output cavity. This plot also shows the most critical regions concerning field emission due to high electric fields on the metal surface.

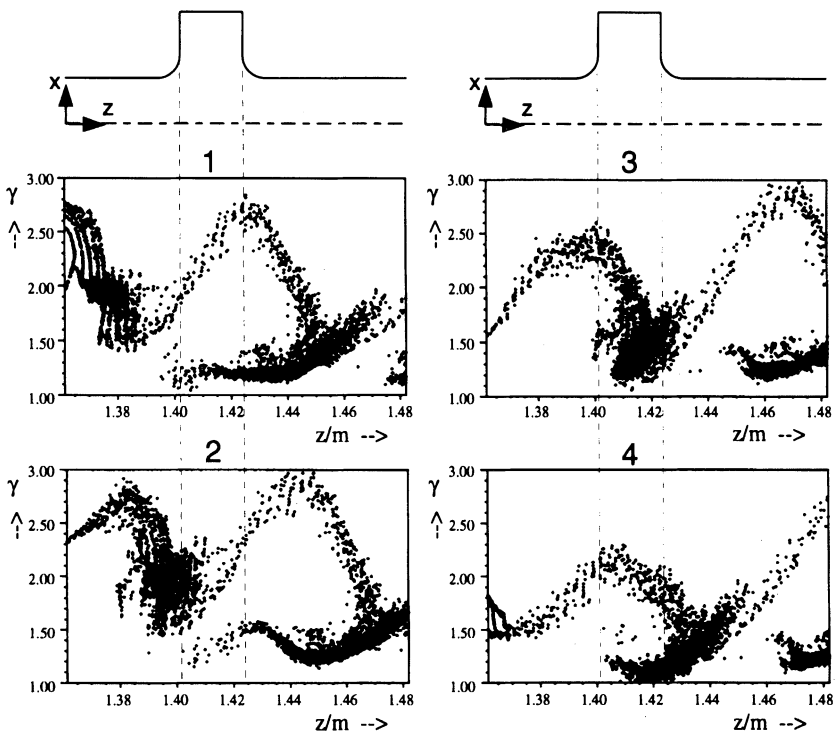

FIGURE 12: The relative mass γ of the macro particles over one RF-period T in the region of the output cavity. The location of the output cavity is shown by the dotted lines. While moving into the cavity core the particles obviously loose most of their kinetic energy.

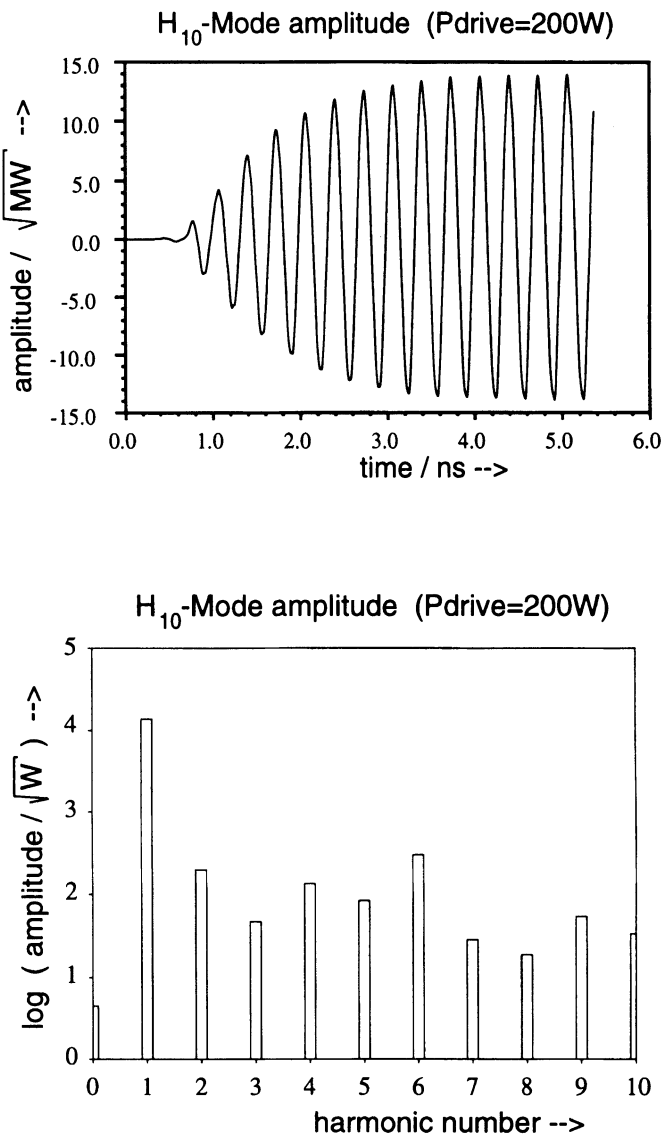

FIGURE 13: The upper plot shows the amplitude of the outgoing fundamental waveguide mode as function of time. Steady state is reached after 15 RF-periods. The Fourier Series of the last two RF-periods is shown in the lower plot. The amplitude at the first harmonic determines the output power extracted through one rectangular waveguide. The second waveguide shows the same behaviour. These plots refer to a drive power of 200 W in the first cavity and a DC-gun voltage of 535 kV.

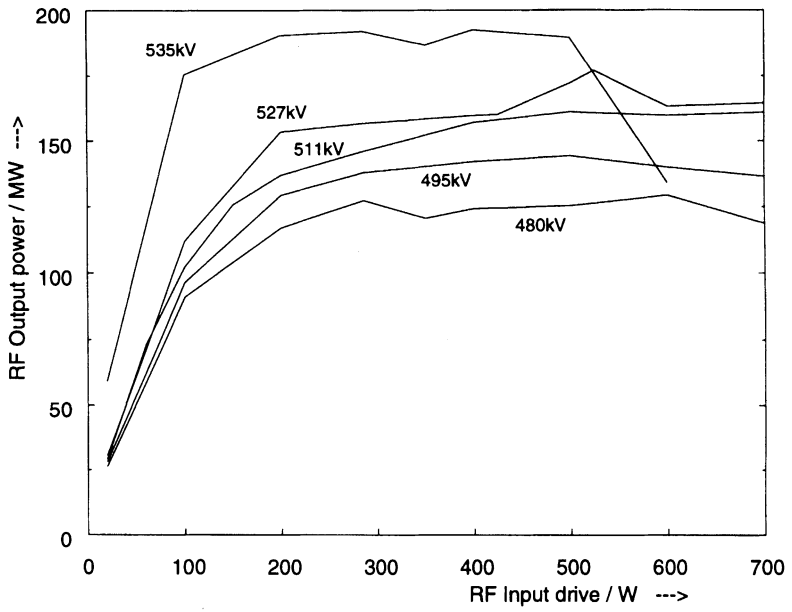

FIGURE 14: This plot shows the RF-power extracted by the first harmonic of the H_{10}-mode through the two rectangular waveguides as function of drive power. The values are calculated using the 3D PIC code MAFIA-TS3. The simulation is performed for five different DC-gun voltages and currents: a) 535 kV/700 A, b) 527 kV/680 A, c) 511 kV/656 A, d) 495 kV/628 A, e) 480 kV/600 A. The following values for the saturated output power have been measured: b) 154 MW, c) 140 MW and d) 133 MW. No measurements are available for the input conditions a) and e).

The structure shown in Figure 8 is discretized with 206,241 meshpoints. Each of the 1065 2D ring charges per RF-period is split into eight point charges. Thus the number of used 3D particles is 8520 per RF-period. The calculation of 15 RF-periods takes 3.6 hours cpu-time on a SUN-SPARC 20 workstation.

A typical time signal of an outgoing fundamental waveguide mode is shown in Figure 13. In the simulations two periods are used for switching-on charge and field ($T_{on} = 2\,T$). The higher harmonics of the driving frequency are extracted by the transformation into the Fourier series as illustrated in Figure 13.

A study on the intercepted current and its power loss in the tube walls is shown in Figure 15.

5 SUMMARY

We presented a 3D PIC simulation of a klystron output circuit for a 150 MW S-band klystron including the realistic extraction of the power through the rectangular waveguides. The simulation takes into account the cavity with all modes and fully relativistic particle dynamics. The assumptions made at the interface plane between 2D and 3D PIC simulation

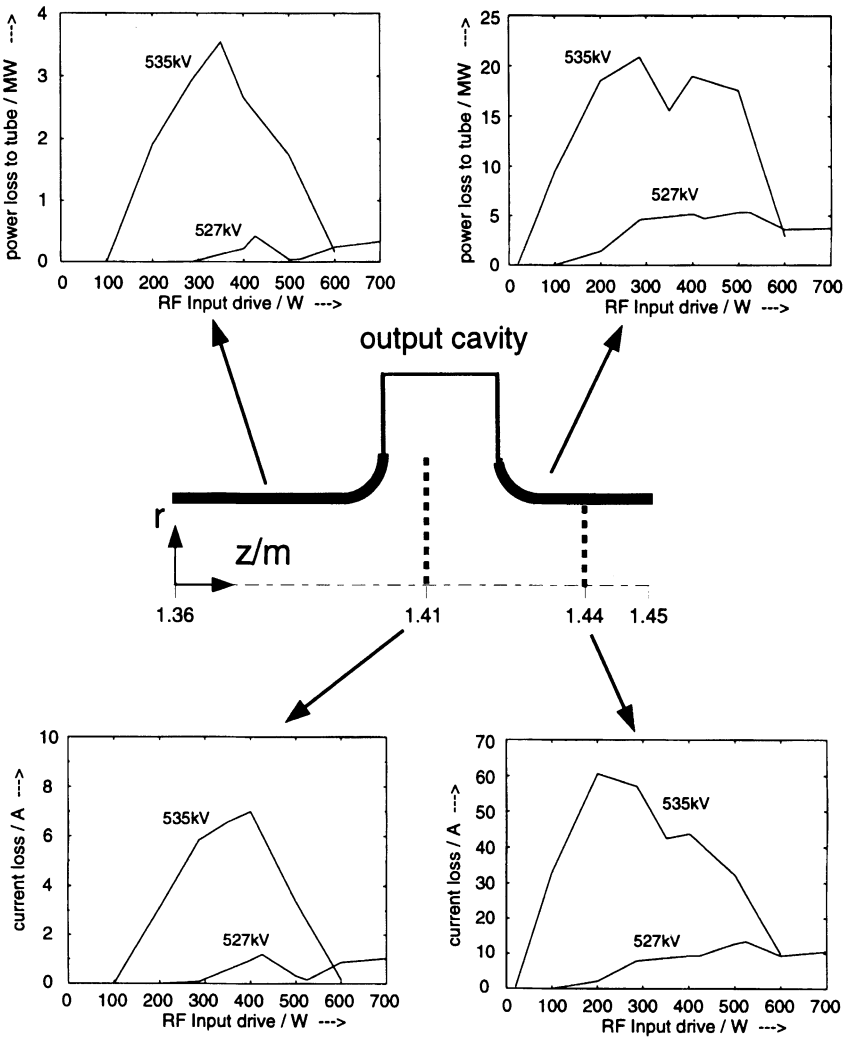

FIGURE 15: This figure illustrates some information on the intercepted current for the DC-gun voltages a) 535 kV and b) 527 kV. In the upper plots the power loss in the tube wall due to hitting particles is shown. The lower pictures show the amount of DC-current loss at two different z-positions (z=1.41 m and z=1.44 m, both measured from cathode center).

have been checked to be fulfilled. The cpu-time (3.6 hours on a SUN-SPARC 20 workstation to simulate 15 RF-periods) and the memory requirement for the particle- and field-interface are quite low. The calculated RF output power as function of the drive level shows good agreement with measurements. A detailed comparison with measurements and simulation results using other 2D klystron codes is presented in Reference 2.

The 3D simulation offers multiple possibilites of postprocessing, e.g. studies on the intercepted current, power loss in the tube wall, deposited energy or surface gradients. Those informations, all including unsymmetrical effects in the output cavity, are very useful for the design of high power klystrons.

ACKNOWLEDGEMENTS

The authors wish to thank all members of the Klystron Department at the Stanford Linear Accelerator Center, where the work was started. For many helpful discussions we thank K. Eppley, T. Shintake and S. Luetgert.

REFERENCES

1. D. Sprehn, R.M. Phillips, G. Caryotakis, *The design and performance of 150-MW S-Band Klystrons*, September 1994, SLAC-PUB-6677.
2. U. Becker, M. Dohlus, S. Lütgert, D. Sprehn, T. Weiland, *Comparison of CONDOR, FCI and MAFIA Calculations for a 150MW S-Band Klystron with Measurements*, Particle Accelerator Conference 1995, Dallas.
3. T. Weiland, *On The Numerical Solution Of Maxwell's Equations And Applications In The Field Of Accelerator Physics*, Particle Accelerators, **15**, 245–292 (1984).
4. W.B. Herrmannsfeldt, *EGUN, An Electron Optics and Gun Design Program*, October 1988, SLAC-Report-331.
5. S. Yu, *Particle-In-Cell Simulation of High Power Klystrons*, September 1984, SLAC/AP-34.
6. K.R. Eppley, *Modelling RF Sources using 2-D PIC Codes*, March 1993, SLAC-PUB-6067.
7. T. Weiland, *Time Domain Electromagnetic Field Computation with the Finite Difference Methods*, IEEE Workshop, Discrete time domain modelling of electromagnetic fields and networks, Berlin, 1993.
8. T. Weiland, *High Precision Eigenmode Computation*, to be submitted to Particle Accelerators.
9. M. Dohlus, P. Thoma, T. Weiland, *Broadband Simulation of Open Waveguide Boundaries within large frequency ranges*, IEEE Workshop, Discrete time domain modelling of electromagnetic fields and networks, Berlin, 1993.
10. C.K. Birdsall, A.B. Langdon, *Plasma Physics via Computer Simulation*, Adam Hilger Book Company, New York 1991.
11. P. Schütt, *Zur Dynamik eines Elektronen-Hohlstrahls*, Dissertation Hamburg, August 1988, DESY M-88-03.
12. O. Buneman, *Relativistic Plasmas*, p. 205, Benjamin, New York, 1968.
13. The MAFIA collaboration, *User's Guide MAFIA Version 3. x*, CST GmbH, Lauteschlägerstr. 38, 64289 Darmstadt, Germany.